METHOD OF EFFECTIVE SECTIONS TO TAKE ACCOUNT OF SELECTIVITY OF RADIATION AND ABSORPTION IN A HOT GAS

V. M. Ovsyannikov

UDC 536.24

A method, economical in computing time, for solving radiation transfer problems by using the integrated characteristics of the absorption spectrum, the effective sections, is elucidated. The shock layer ahead of a body around which a hypersonic gas flows is analyzed in the presence of intensive mass delivery from the surface. The machine time in the computational examples is shortened 120-fold as compared with an exact computation, and the error in calculating the radiation fluxes does not exceed 15-25%.

1. Method of Effective Sections

Let us consider radiation transfer in a domain filled with a selectively radiating and absorbing hot gas. We do not take scattering into account. Under the assumption of local thermodynamic equilibrium, the emission of radiation by a radiation flux and its divergence at a point with coordinate $\mathbf{r}$ are

$$q(\mathbf{r}) = \int_{(\omega)} d\omega \cos\theta \int_{(\Delta\lambda)} d\lambda \int_{\mathbf{r}}^{\mathbf{r}_1(\omega)} B_\lambda(T(\mathbf{r}')) \exp[-t_\lambda(\mathbf{r}, \mathbf{r}')] N(\mathbf{r}') \sigma_\lambda(\mathbf{r}')\, d\mathbf{r}'$$

$$\operatorname{div} q(\mathbf{r}) = \int_{(\Delta\lambda)} d\lambda k_\lambda(\mathbf{r}) \left\{ \int_{(\omega)} d\omega \int_{\mathbf{r}}^{\mathbf{r}_1(\omega)} B_\lambda(T(\mathbf{r}')) \exp[-t_\lambda(\mathbf{r}, \mathbf{r}')] N(\mathbf{r}') \sigma_\lambda(\mathbf{r}')\, d\mathbf{r}' - 4\pi B_\lambda(T(\mathbf{r})) \right\} \tag{1.1}$$

$$t_\lambda(\mathbf{r}, \mathbf{r}') = \int_{\mathbf{r}}^{\mathbf{r}'} N(\mathbf{r}'') \sigma_\lambda(\mathbf{r}'')\, d\mathbf{r}''$$

Here $d\mathbf{r}''$ is the differential of the length along the ray $(\mathbf{r}, \mathbf{r}')$, λ is the wavelength, $(\Delta\lambda)$ is the wavelength band within which the radiation must be taken into account, T is the temperature, N is the number of particles per unit volume, ω is a three-dimensional angle measured from the initial direction e (see Fig. 1a), θ is the angle between the ray direction and the normal $\mathbf{e}_1$ to the area under consideration, $\mathbf{r}_1(\omega)$ is a point on the boundary of the radiating volume, k_λ is the reduced volume coefficient of absorption taking forced emission into account, σ_λ is the absorption cross section, $B_\lambda(T)$ is the Planck function of equilibrium radiation, and π is the ratio of the circumference to the diameter.

For gas mixtures heated to 2000-20,000°K temperatures, the absorption section σ_λ is a complex function of the wavelength containing the continuous spectrum, the molecular bands, the atomic and ionic lines. The absorption section of the mixture depends on the component concentration and is a function of the temperature and other parameters for each component. Integration over the wavelength should be carried out with a fine spacing; hence, the use of (1.1) results in large machine-time expenditures.

Integration over λ in the method of effective sections is carried out beforehand, separately from the calculation of the field of radiation fluxes. Let us introduce the effective sections s, σ, ε:

$$s(\mathbf{r}, \mathbf{r}') = s(T(\mathbf{r}'), N(\mathbf{r} - \mathbf{r}'), \sigma_\lambda(\mathbf{r} - \mathbf{r}')) = \int_{(\Delta\lambda)} d\lambda B_\lambda^\circ(T(\mathbf{r}')) \sigma_\lambda(\mathbf{r}') \sigma_\lambda(\mathbf{r}) \exp\left[-\int_{\mathbf{r}}^{\mathbf{r}'} N(\mathbf{r}'') \sigma_\lambda(\mathbf{r}'')\, d\mathbf{r}''\right]$$

Moscow. Translated from Zhurnal Prikladnoi Mekhaniki i Tekhnicheskoi Fiziki, No. 5, pp. 76-83, September-October, 1972. Original article submitted May 17, 1972.

$$\sigma(\mathbf{r}, \mathbf{r}') = \sigma(T(\mathbf{r}'), N(\mathbf{r}-\mathbf{r}'), \sigma_\lambda(\mathbf{r}-\mathbf{r}')) = \int\limits_{(\Delta\lambda)} d\lambda B_\lambda^\circ(T(\mathbf{r}'))\sigma_\lambda(\mathbf{r}')\exp\left[-\int\limits_{\mathbf{r}}^{\mathbf{r}'} N(\mathbf{r}'')\sigma_\lambda(\mathbf{r}'')\,d\mathbf{r}''\right] \tag{1.2}$$

$$\varepsilon(T, N(\mathbf{r}-\mathbf{r}'), \sigma_\lambda(\mathbf{r}-\mathbf{r}')) = \int\limits_{(\Delta\lambda)} d\lambda B_\lambda^\circ(T)\left\{1-\exp\left[-\int\limits_{\mathbf{r}}^{\mathbf{r}'} N(\mathbf{r}'')\sigma_\lambda(\mathbf{r}'')\,d\mathbf{r}''\right]\right\}$$

$$B_\lambda^\circ(T) = B_\lambda(T)/B(T), \quad B(T) = (\sigma^\circ/\pi)T^4$$

where σ° is the Stefan–Boltzmann constant. The radiation flux and its divergence (1.1) are expressed in terms of the effective sections:

$$q(\mathbf{r}) = \int\limits_{(\omega)} d\omega\cos\theta \int\limits_{\mathbf{r}}^{\mathbf{r}_1(\omega)} B(T(\mathbf{r}'))\sigma(\mathbf{r}, \mathbf{r}')N(\mathbf{r}')\,d\mathbf{r}'$$

$$\operatorname{div} q(\mathbf{r}) = N(\mathbf{r})\int\limits_{(\omega)} d\omega \int\limits_{\mathbf{r}}^{\mathbf{r}_1(\omega)} B(T(\mathbf{r}'))s(\mathbf{r}, \mathbf{r}')N(\mathbf{r}')\,d\mathbf{r}' - 4\pi B(T(\mathbf{r}))\sigma_p(\mathbf{r})N(\mathbf{r})$$

$$\sigma_p(\mathbf{r}) = \sigma_p(T(\mathbf{r}), \sigma_\lambda(\mathbf{r})) = \int\limits_{(\Delta\lambda)} d\lambda B_\lambda^\circ(T(\mathbf{r}))\sigma_\lambda(\mathbf{r}) \tag{1.3}$$

Here σ_p is the mean Planck absorption section. The absorption section ε will be introduced in the expression for the radiation flux in Section 2. There is no integration over the wavelength in (1.3); hence their application yields a great saving in computation time as compared with the use of (1.1). Information about the spectrum characteristics of the gas is contained in the effective sections, which are interconnected by the relations

$$\frac{d\varepsilon(T, \mathbf{r}-\mathbf{r}')}{d\mathbf{r}'} = N(\mathbf{r}')\sigma(T, \mathbf{r}-\mathbf{r}'), \quad \frac{d\sigma(\mathbf{r}, \mathbf{r}')}{d\mathbf{r}} = -N(\mathbf{r})s(\mathbf{r}, \mathbf{r}') \tag{1.4}$$

$$\varepsilon(T, \mathbf{r}-\mathbf{r}') = \int\limits_{\mathbf{r}}^{\mathbf{r}'}\sigma(T, \mathbf{r}-\mathbf{r}'')N(\mathbf{r}'')\,d\mathbf{r}'', \quad \sigma(\mathbf{r}, \mathbf{r}') = \sigma_p(\mathbf{r}') - \int\limits_{\mathbf{r}}^{\mathbf{r}'} s(\mathbf{r}'', \mathbf{r}')N(\mathbf{r}'')\,d\mathbf{r}''$$

In the general case when the absorption section σ_λ varies arbitrarily along the coordinate $\mathbf{r}$, the effective sections s, σ, ε are functionals dependent on the functions N and σ_λ in the interval $(\mathbf{r}, \mathbf{r}')$ and on the temperature at the point $\mathbf{r}'$. The effective sections are functions for dependences of the absorption section on a specific kind of coordinate and can be calculated in advance.

Let the absorption section be a function of the wavelength and temperature of the form

$$\sigma_\lambda(T) = \sum_{k=1}^{\varkappa}\psi_k(T)S_k(\lambda) \tag{1.5}$$

For instance, if the absorption section σ_λ is given for the temperatures $T_1, \ldots, T_\varkappa$ and linear interpolation in the values $\sigma_\lambda(T_k)$ and $\sigma_\lambda(T_{k+1})$ is used to obtain the values of σ_λ at the intermediate temperatures $T_k < T < T_{k+1}$ $(k = 1, \ldots, \varkappa-1)$, then

$$S_k(\lambda) = \sigma_\lambda(T_k) \quad (k = 1, \ldots, \varkappa) \tag{1.6}$$

$$\begin{gathered}\psi_k = (T_{k+1}-T)/(T_{k+1}-T_k) \text{ for } T_k \leqslant T < T_{k+1} \\ \psi_k = (T-T_{k-1})/(T_k-T_{k-1}) \text{ for } T_{k-1} < T < T_k \\ \psi_k = 0 \text{ for } T \leqslant T_{k-1}, \ T \geqslant T_{k+1} \quad (k = 2, \ldots, \varkappa-1)\end{gathered} \tag{1.7}$$

$$\begin{gathered}\psi_1 = (T_2-T)/(T_2-T_1) \text{ for } T_1 < T < T_2, \\ \psi_1 = 1 \text{ for } T \leqslant T_1, \ \psi_1 = 0, \text{ for } T \geqslant T_2 \\ \psi_\varkappa = (T-T_{\varkappa-1})/(T_\varkappa-T_{\varkappa-1}) \text{ for } T_{\varkappa-1} < T, \\ \psi_\varkappa = 0 \text{ for } T \leqslant T_{\varkappa-1}, \ \psi_\varkappa = 1 \text{ for } T \geqslant T_\varkappa\end{gathered} \tag{1.8}$$

Let us introduce the functions $n_k(\mathbf{r}, \mathbf{r}')$ which equal the number of particles allotted to the absorption section $\sigma_\lambda(T_k)$ on the ray $(\mathbf{r}, \mathbf{r}')$ with unit cross section:

$$n_k(\mathbf{r}, \mathbf{r}') = \int\limits_{\mathbf{r}}^{\mathbf{r}'} N(\mathbf{r}'')\psi_k(T(\mathbf{r}''))\,d\mathbf{r}''$$

$$t_\lambda(\mathbf{r}', \mathbf{r}) = \int\limits_{\mathbf{r}}^{\mathbf{r}'} N(\mathbf{r}'')\sigma_\lambda(T(\mathbf{r}''))\,d\mathbf{r}'' = \sum_{k=1}^{\varkappa} S_k(\lambda)n_k(\mathbf{r}, \mathbf{r}')$$

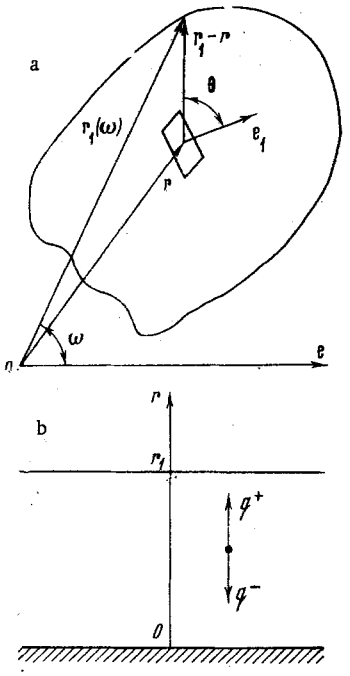

Fig. 1

The expressions for q(r), div q(r) in (1.3) and the effective sections in (1.2) become

$$q(\mathbf{r}) = \int_{(\omega)} d\omega \cos\theta \sum_{k=1}^{\varkappa} \int_{r}^{r_1(\omega)} B(T(\mathbf{r}'))\, \sigma_k(T(\mathbf{r}'), n_1(\mathbf{r}, \mathbf{r}'), \ldots, n_\varkappa(\mathbf{r}, \mathbf{r}'))\, dn_k(r')$$

$$\operatorname{div} q(\mathbf{r}) = \sum_{k=1}^{\varkappa} N(\mathbf{r})\, \psi_k(T(\mathbf{r})) \Big\{ \int_{(\omega)} d\omega \sum_{i=1}^{\varkappa} \int_{r}^{r_1(\omega)} dn_i(\mathbf{r}')\, B(T(\mathbf{r}')) \times \Big.$$

$$\Big. \times s_{ki}(T(\mathbf{r}'), n_1(\mathbf{r}, \mathbf{r}'), \ldots, n_\varkappa(\mathbf{r}, \mathbf{r}')) - 4\pi B(T(\mathbf{r}))\, \sigma_k(T(\mathbf{r}), 0, \ldots, 0) \Big\},$$

$$dn_k(\mathbf{r}') = N(\mathbf{r}')\, \psi_k(T(\mathbf{r}'))\, dr' \qquad (1.9)$$

$$s_{ki}(T, n_1, \ldots, n_\varkappa) = \int_{(\Delta\lambda)} d\lambda B_\lambda^\circ(T)\, S_k(\lambda) S_i(\lambda) \exp\Big(-\sum_{j=1}^{\varkappa} S_j(\lambda) n_j\Big)$$

$$\sigma_k(T, n_1, \ldots, n_\varkappa) = \int_{(\Delta\lambda)} d\lambda B_\lambda^\circ(T)\, S_k(\lambda) \exp\Big(-\sum_{j=1}^{\varkappa} S_j(\lambda) n_j\Big) \qquad (1.10)$$

$$\varepsilon(T, n_1, \ldots, n_\varkappa) = \int_{(\Delta\lambda)} d\lambda B_\lambda^\circ(T) \Big[1 - \exp\Big(-\sum_{j=1}^{\varkappa} S_j(\lambda) n_j\Big)\Big]$$

For a homogeneous gas with σ_λ independent of the temperature, $n_1(\mathbf{r}, \mathbf{r}')$ is the number of particles in the segment $(\mathbf{r}, \mathbf{r}')$ of a ray with unit cross section. If the temperature T is constant in the domain under consideration, then $\varepsilon(T, n_1)$ is the degree of blackness of a cone with unit solid angle for which a ray with unit cross section directed along the altitude contains n_1 particles. In conformity with the first relation (1.4), the effective section $\sigma(T, n_1)$ equals the change in the degree of blackness of the mentioned cone as n_1 changes by one. For $n_1 = 0$ the value of $\sigma(T, 0)$ equals the mean section of Planck absorption.

It is sufficient to know one of the three functions s, σ, ε for the characteristics of the optical properties of the gas and to obtain the rest by using (1.4). However, in order to avoid errors associated with transforming the function given at discrete points, it is necessary to calculate each effective section by means of (1.10).

The number of functions of the wavelength $S_k(\lambda)$ to be used to construct the optical model (1.5) of a homogeneous gas will be called the order of the approximation $\varkappa$ of the method of effective sections. The first approximation of the method was proposed in papers of Thompson and Penner elucidated in [1] and used in a number of papers to compute a plane radiating layer.

2. Plane Layer

Let us consider a plane gas layer with a uniform temperature distribution. The origin lies on the layer boundary (see Fig. 1b). The expressions for the radiation flux q, its divergence, and one-sided fluxes q^+, q^-

$$q(r) = q^+(r) - q^-(r)$$

$$q^+(r) = \int_{(\Delta\lambda)} d\lambda \int_0^r B_\lambda(T(r'))\, 2E_2[t_\lambda(r', r)]\, N(r')\, \sigma_\lambda(r')\, dr'$$

$$q^-(r) = \int_{(\Delta\lambda)} d\lambda \int_r^{r_1} B_\lambda(T(r'))\, 2E_2[t_\lambda(r, r')]\, N(r')\, \sigma_\lambda(r')\, dr'$$

$$\operatorname{div} q(r) = \int_{(\Delta\lambda)} d\lambda k_\lambda(r) \Big\{ \int_0^{r_1} \pi B_\lambda(T(r'))\, 2E_1[t_\lambda(r, r')]\, N(r')\, \sigma_\lambda(r')\, dr' - 4\pi B_\lambda(T(r)) \Big\}$$

become under the assumption (1.5)

$$q^-(r) = \pi B(T(r))\, \varepsilon^*(T(r), n_1(r, r+\delta), \ldots, n_\varkappa(r, r+\delta)) +$$

$$+ \sum_{k=1}^{\varkappa} \int_{r+\delta}^{r_1} \pi B(T(r'))\, \sigma_k^*(T(r'), n_1(r, r'), \ldots, n_\varkappa(r, r'))\, dn_k(r')$$

$$q^+(r) = \pi B(T(r))\, \varepsilon^*(T(r), n_1(r-\delta, r), \ldots, n_\varkappa(r-\delta, r)) + \qquad (2.1)$$

$$+ \sum_{k=1}^{\varkappa} \int_0^{r-\delta} \pi B(T(r'))\, \sigma_k^*(T(r'), n_1(r, r'), \ldots, n_\varkappa(r, r'))\, dn_k(r')$$

$$\operatorname{div} q(r) = -2\pi B(T(r))\,N(r)\sum_{k=1}^{\varkappa}\psi_k(T(r))\,\sigma_k^*(T(r),\ n_1(r,\ r+\delta),\ldots,n_\varkappa(r,\ r+\delta))$$
$$+N(r)\left\{\int_0^{r-\delta}\pi B(T(r'))\sum_{k=1}^{\varkappa}\psi_k(T(r))\sum_{i=1}^{\varkappa}s_{ki}^*(T(r'),\ n_1(r,\ r'),\ldots\right.$$
$$\left.\ldots,\ n_\varkappa(r,\ r'))\,dn_i(r')+\int_{r+\delta}^{r_1}\pi B(T(r'))\sum_{k=1}^{\varkappa}\psi_k(T(r))\sum_{i=1}^{\varkappa}s_{ki}^*(T(r'),\ n_1(r,\ r'),\ldots\right.$$
$$\left.\ldots,n_\varkappa(r,\ r'))\,dn_i(r')\right\} \tag{2.2}$$

The effective sections in the plane case are

$$s_{ki}^*(T,\ n_1,\ldots,n_\varkappa)=\int_{(\Delta\lambda)}d\lambda B_\lambda^\circ(T)\,S_k(\lambda)\,S_i(\lambda)\,2E_1\left(\sum_{j=1}^{\varkappa}S_j(\lambda)\,n_j\right)$$
$$\sigma_k^*(T,\ n_1,\ldots,n_\varkappa)=\int_{(\Delta\lambda)}d\lambda B_\lambda^\circ(T)\,S_k(\lambda)\,2E_2\left(\sum_{j=1}^{\varkappa}S_j(\lambda)\,n_j\right) \tag{2.3}$$
$$\varepsilon^*(T,\ n_1,\ldots,n_\varkappa)=\int_{(\Delta\lambda)}d\lambda B_\lambda^\circ(T)\left[1-2E_3\left(\sum_{j=1}^{\varkappa}S_j(\lambda)\,n_j\right)\right]$$

Here E_1, E_2, E_3 are exponential integral functions of the first, second and third orders.

It was assumed in deriving (2.1), (2.2) that the temperature varies sufficiently smoothly over the coordinate r so that at points a distance δ apart the Planck function $B_\lambda(T)$ can be considered independent of the coordinate within the limits of admissible error. The first term on the right side of the equalities in the formulas for q^-, q^+ (2.1) is the radiation from an isothermal plane layer of thickness δ. The use of ε^* in (2.1) and σ_k^* ($k=1,\ldots,\varkappa$) in (2.2) permits shortening the volume of the table of effective sections needed to solve the problem. The effective sections in (1.9) must be known for the values of n_k corresponding to intervals between 0 and the maximum size of the domain which we denote by d. The effective sections for values of n_k corresponding to smaller intervals between δ and d are used in (2.1), (2.2). The ratio d/δ is usually 10-40 in radiation transfer problems; hence the effective sections must be known as n_k varies approximately 10-40-fold.

For a plane layer, the relations (1.4) become under the assumption (1.5)

$$\partial\varepsilon^*/\partial n_k=\sigma_k^*,\quad \partial\sigma_k^*/\partial n_i=-s_{ki}^*$$
$$\sigma_k^*=\left[\sigma_k^*(T,\ 0,\ldots,0)-\sum_{i=1}^{\varkappa}\int_0^{n_i}s_{ik}^*\,dn_i\right],\ \varepsilon^*=\sum_{k=1}^{\varkappa}\int_0^{n_k}\sigma_k^*\,dn_k\quad(k=1,\ldots,\varkappa)$$

3. Multicomponent Mixture

Let the mixture contain $\varkappa$ components with molar concentrations x_k ($k=1,\ldots,\varkappa$). The temperature dependence of the absorption section of each component $\sigma_{\lambda k}$ ($k=1,\ldots,\varkappa$) will be represented as

$$\sigma_{\lambda k}(T)=\varphi_k(T)S_k(\lambda)$$

i.e., we use the assumption of the first approximation of the method of effective sections for a homogeneous gas. Let the absorption section of the mixture be calculated by means of the formula

$$\sigma_\lambda(T,\ x_1,\ldots,x_\varkappa)=\sum_{k=1}^{\varkappa}x_k\sigma_{\lambda k}(T)$$

If the number of particles allotted to the absorption section $S_k(\lambda)$ on a ray (r, r') with unit cross section is calculated as

$$n_k(r,\ r')=\int_r^{r'}N(r'')\,x_k(r'')\,\varphi_k(T(r''))\,dr''\quad(k=1,\ldots,\varkappa)$$

then the radiation flux and its divergence in a multicomponent mixture can be calculated by formulas of the $\varkappa$-th approximation of the homogeneous gas (1.9), (1.10) in the three-dimensional and (2.1)-(2.3) in the plane cases if we put $\psi_k=x_k\varphi_k(T)$ therein.

TABLE 1

$10^{-18}n_1$, cm^{-2}	T, °K										
	9000		10000		11000		12000		13000		
	a	b	a	b	a	b	a	b	a	b	
10^{-2}	0.572	−2	0.235	−1	0.740	−1	0.190	0	0.421	0	
10^{-1}	0.169	−2	0.626	−2	0.181	−1	0.436	−1	0.909	−1	
1	0.227	−3	0.425	−3	0.879	−3	0.171	−2	0.300	−2	
10	0.518	−4	0.434	−4	0.386	−4	0.373	−4	0.392	−4	
10^2	0.653	−5	0.553	−5	0.475	−5	0.412	−5	0.361	−5	$10^{36}s^*$, cm^4
10^3	0.289	−6	0.282	−6	0.274	−6	0.265	−6	0.256	−6	
10^4	0.510	−9	0.644	−9	0.772	−9	0.889	−9	0.990	−9	
0	0.463	−2	0.620	−2	0.111	−1	0.219	−1	0.420	−1	
10^{-4}	0.463	−2	0.619	−2	0.111	−1	0.218	−1	0.419	−1	
10^{-3}	0.462	−2	0.615	−2	0.109	−1	0.215	−1	0.411	−1	
10^{-2}	0.455	−2	0.588	−2	0.101	−1	0.193	−1	0.362	−1	$10^{18}\sigma^*$, cm^2
10^{-1}	0.426	−2	0.482	−2	0.692	−2	0.115	−1	0.194	−1	
1	0.374	−2	0.346	−2	0.351	−2	0.396	−2	0.486	−2	
10	0.288	−2	0.252	−2	0.223	−2	0.200	−2	0.182	−2	
10^2	0.140	−2	0.129	−2	0.120	−2	0.111	−2	0.104	−2	
10^3	0.240	−3	0.250	−3	0.256	−3	0.261	−3	0.263	−3	
10^4	0.119	−5	0.153	−5	0.187	−5	0.218	−5	0.246	−5	
0	0	0	0	0	0	0	0	0	0	0	
10^{-4}	0.465	−6	0.622	−6	0.111	−5	0.219	−5	0.421	−5	
10^{-3}	0.464	−5	0.620	−5	0.110	−4	0.218	−4	0.417	−4	
10^{-2}	0.460	−4	0.604	−4	0.105	−3	0.204	−3	0.388	−3	
10^{-1}	0.441	−3	0.533	−3	0.839	−3	0.150	−2	0.270	−2	ε^*
1	0.398	−2	0.401	−2	0.483	−2	0.679	−2	0.103	−1	
10	0.329	−1	0.295	−1	0.280	−1	0.287	−1	0.320	−1	
10^2	0.204	0	0.183	0	0.167	0	0.156	0	0.149	0	
10^3	0.696	0	0.664	0	0.636	0	0.613	0	0.594	0	
10^4	0.979	0	0.978	0	0.977	0	0.977	0	0.976	0	
10^5	0.982	0	0.982	0	0.982	0	0.982	0	0.983	0	

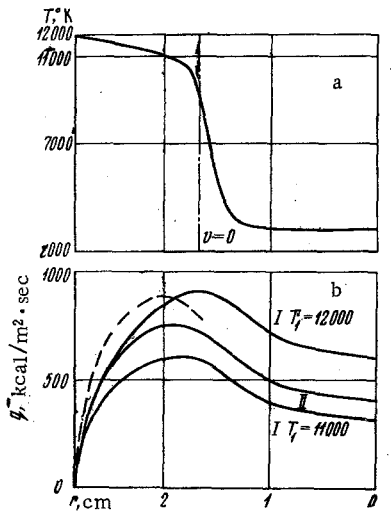

Fig. 2

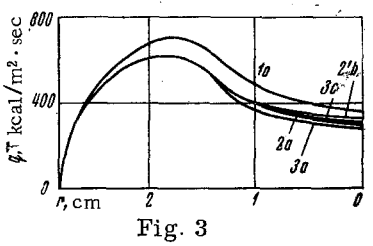

Fig. 3

4. Numerical Computations of the Shock Layer

Effective sections were calculated for the continuous spectrum of air in the first and second approximations. The absorption coefficients were taken from the book [2].

Presented in Table 1 are the effective sections of air in a first approximation for a plane layer in the form $a \cdot 10^b$.

The absorption section was considered temperature independent and equal to the absorption section at a 12,000°K temperature and 1 atm pressure.

For a small optical thickness the effective sections s, σ, s*, σ^* tend to constant values, and ε, ε^* become linear functions of n_1:

$$\sigma \to \sigma(T, 0), \quad \sigma^* \to 2\sigma(T, 0), \quad s \to s(T, 0), \quad s^* \to 2s(T, 0)$$
$$\varepsilon \to n_1\sigma(T, 0), \quad \varepsilon^* \to n_1\sigma^*(T, 0) = 2n_1\sigma(T, 0) = 2n_1\sigma_p \text{ for } n_1 \to 0$$

Linear interpolation (1.6), (1.8) with $T_1 = 11{,}000$°K, $T_2 = 12{,}000$°K was used to calculate the effective sections of air in a second approximation.

The problem of radiation transfer in the shock layer of a sphere around which a hypersonic air stream flowed was solved by the method of effective sections. The computations were carried out on the critical line under intense gas injection through the body surface. The profile of the velocity normal to the body surface was assumed linear. The ordinary differential equation of heat influx taking account of heat conductivity, radiation and absorption was solved by the factorization method in the one-dimensional plane layer approximation.

Let us compare the radiation flux calculated by the method of effective sections with the flux calculated exactly for the temperature profile in the shock layer pictured in Fig. 2a. The coordinate at which the gas velocity normal to the body surface vanishes (v = 0) is denoted by the vertical dash-dot line. A boundary layer where viscosity, heat conductivity, and diffusion processes exist is in the neighborhood of this

TABLE 2

T, °K				$10^{-18} n_1$, cm^{-2}					
a	b	c		1	2	2′		3	
11 000	8 000	3 000	9 000	0	0	0	10	0	1
12 000	9 000	5 000	10 000	0.05	0.05	10^{-4}	10^{2}	0.05	2.5
	10 000	6 000	11 000	20	0.5	10^{-3}	10^{3}	0.1	5
	11 000	7 000	12 000		5	10^{-2}	10^{4}	0.25	10
	12 000	8 000			20	10^{-1}	10^{5}	0.5	20

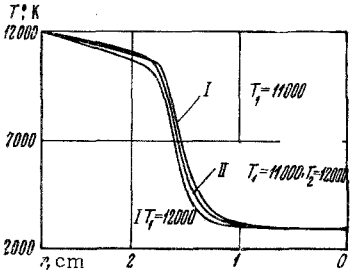

Fig. 4

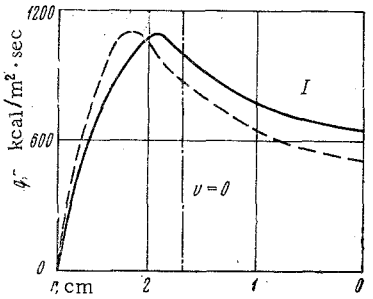

Fig. 5

line. Mixing of the injected gas with the air from the exterior stream which has passed through the shockwave occurs in the same neighborhood, and the thickness of the diffusion layer agrees approximately with the thickness of the heat conductivity layer. Diffusion was not taken into account in the model under consideration, and it was assumed that there is air to the left of the line v = 0 and injected gas to the right. The pressure across the shock layer was assumed constant, equal to 1 atm. The injected gas has the optical characteristics of air in the computations presented in Figs. 2-4.

A dependence of the one-sided radiation flux towards the body $q^-(r)$ on the coordinate is presented in Fig. 2b. The dashed line shows the result of an exact computation, while the solid lines are by the method of effective sections. The Roman numeral indicates the number of the approximation and the value of the characteristic temperature T_1 for which the absorption section was taken in computing the effective sections in a first approximation. In the second approximation $T_1 = 11{,}000°K$, $T_2 = 12{,}000°K$. The solution in the first approximation with $T_1 = 12{,}000°K$ is a better approximation to the exact computation than with $T_1 = 11{,}000°K$. This is explained by the fact that ~80% of the radiation flux is produced by the outer part of the shock layer with the 11,500°K temperature. The solution in the second approximation lies between the first approximation solutions with $T_1 = 11{,}000°K$ and $T_1 = 12{,}000°K$. The accuracy of the radiation flux calculation in the first approximation with $T_1 = 12{,}000°K$ is 14% and in the second approximation is 20%. However, a picture of the change in q^- with r in the second approximation agrees better with the exact picture, and the point of reaching maximum q^- in the second approximation lies closer to the maximum of the exact curve than in the first approximation. The time to compute one iteration of the temperature profile is 25 min when using a difference scheme with 26 points for the exact calculation and 13 sec when using the method of effective sections, i.e., approximately 1/120 of the time.

The investigation of the influence of the spacing of the effective-section tables on the accuracy of computing the radiation flux q^- across the shock layer is represented in Fig. 3. Effective sections in a first approximation were used for $T_1 = 11{,}000°K$ with the n_1 and T spacing presented in Table 2. Intermediate values were determined by linear interpolation of the logarithms of the effective sections in the logarithms of T and n_1. The numbers and letters on the curves in Fig. 3 denote the version of the nodal point arrangement on the effective-section tables. The nodal arrangement 2′b, assuring an error not greater than 3% in comparison with the most exact arrangement 3c, is optimal. The optimal mesh has nodal values in n_1 varying tenfold and in temperature at T_1-3000, T_1-2000, T_1-1000, T_1, T_1+1000. The gas domains with temperature below $T_1-3000°K$ yield a negligible contribution to the radiation and work mainly on absorption. The magnitude of the effective sections at low temperatures does not influence the radiation flux profile. Table 1 has the optimal spacing.

Because of the comparatively low air temperature ~12,000°K and the low value of the emitted radiant energy in comparison with the stagnation enthalpy, the temperature profile depends weakly on the spectrum model used. Presented in Fig. 4 are temperature profiles calculated by using effective sections in first and second approximations. Values of the characteristic temperatures T_1 and T_2 used are indicated here. The temperature difference in the major part of the shock layer is not more than 7% and exceeds this value in a narrow thermal boundary layer zone. The computation time is ~1 min while the computation of the temperature profile by the exact method requires a 2 hr machine time expenditure. Therefore,

the method of effective sections can be used to find the temperature profile in radiation gas dynamics problems, and the final radiation flux distribution can be carried out either by the same or by the exact method.

Presented in Fig. 5 is the radiation flux distribution $q^{-}(r)$ in the shock layer with the injection of a gas with optical properties different from air. The dashed curve shows the exact profile, and the solid line is the profile obtained by using the first approximation of the method of effective sections for a binary mixture of air ($T_1 = 12{,}000°K$)-injected gas ($T_2 = 3000°K$). The difference in the radiation fluxes coming in to the wall is 25%.

The author is grateful to G. A. Tirskii for supervising the research and to É. S. Filippov for aid in carrying out the computations.

LITERATURE CITED

1. S. S. Penner, Quantitative Molecular Spectroscopy and Gas Emissivities, Addison-Wesley, Reading, Mass. (1959).
2. V. A. Kamenshchikov, Yu. A. Plastinin, V. M. Nikolaev, and L. A. Novitskii, Radiation Properties of Gases at High Temperatures [in Russian], Mashinostroenie, Moscow (1971).